AD_____

Award Number: DAMD17-03-1-0245

TITLE: Computerized Interpretation of Dynamic Breast MRI

PRINCIPAL INVESTIGATOR: Weijie Chen

CONTRACTING ORGANIZATION: Chicago University
Chicago, Illinois 60637

REPORT DATE: May 2004

TYPE OF REPORT: Annual Summary

PREPARED FOR: U.S. Army Medical Research and Materiel Command
Fort Detrick, Maryland 21702-5012

DISTRIBUTION STATEMENT: Approved for Public Release;
Distribution Unlimited

The views, opinions and/or findings contained in this report are those of the author(s) and should not be construed as an official Department of the Army position, policy or decision unless so designated by other documentation.

REPORT DOCUMENTATION PAGE

Form Approved
OMB No. 074-0188

1. AGENCY USE ONLY (Leave blank)	2. REPORT DATE	3. REPORT TYPE AND DATES COVERED
	May 2004	Annual Summary (14 Apr 2003 - 13 Apr 2004)

4. TITLE AND SUBTITLE
Computerized Interpretation of Dynamic Breast MRI

5. FUNDING NUMBERS
DAMD17-03-1-0245

6. AUTHOR(S)
Weijie Chen

7. PERFORMING ORGANIZATION NAME(S) AND ADDRESS(ES)
Chicago University
Chicago, Illinois 60637

E-Mail: weijie@uchicago.edu

8. PERFORMING ORGANIZATION REPORT NUMBER

9. SPONSORING / MONITORING AGENCY NAME(S) AND ADDRESS(ES)
U.S. Army Medical Research and Materiel Command
Fort Detrick, Maryland 21702-5012

10. SPONSORING / MONITORING AGENCY REPORT NUMBER

11. SUPPLEMENTARY NOTES

12a. DISTRIBUTION / AVAILABILITY STATEMENT
Approved for Public Release; Distribution Unlimited

12b. DISTRIBUTION CODE

13. ABSTRACT (Maximum 200 Words)

One of the most important obstacles of clinical application of breast MRI is the lack of standardization in terms of interpretation guidelines. The purpose of the proposed research is to develop computerized methods to take full advantage of the wealth information that dynamic MRI of the breast offers to improve methods for the diagnosis and prognosis of breast cancer. The research involves investigation of automatic methods for image artifacts correction, tumor segmentation, and extraction of computerized features that help distinguish between benign and malignant lesions. During the first year, we have collected and maintained a dynamic breast MRI database that is well suitable for the proposed research on computerized interpretation of breast MR images. We have developed computerized methods for correction of shading artifacts, tumor segmentation, and feature extraction. The results have shown that computerized analysis and interpretation methods have great promise in increasing the objectivity, efficiency, and accuracy of the diagnosis of breast cancer.

14. SUBJECT TERMS
Feature extraction, tumor segmentation, fuzzy c-means, database

15. NUMBER OF PAGES
28

16. PRICE CODE

17. SECURITY CLASSIFICATION OF REPORT	18. SECURITY CLASSIFICATION OF THIS PAGE	19. SECURITY CLASSIFICATION OF ABSTRACT	20. LIMITATION OF ABSTRACT
Unclassified	Unclassified	Unclassified	Unlimited

Table of Contents

INTRODUCTION

The promising potential of MRI in diagnosis of breast cancer, as a complementary modality to X-ray mammography, has been well recognized [1][2][3]. Contrast-enhanced (CE) MRI is regarded as the most sensitive technique for breast cancer detection; in addition, it is extraordinarily useful in assessing the tumor extent and assessing the therapy response. Despite its well-recognized utilities, however, the technique has not been introduced to routine clinical breast imaging. One of the most important obstacles is the lack of standardization in terms of interpretation guidelines [2][4]. The reproducibility, effectiveness and relative significance of interpretation criteria in the literature are far from being well evaluated. The purpose of the proposed research is to develop computerized methods to take full advantage of the wealth information that dynamic MRI offers to improve methods for the diagnosis and prognosis of breast cancer. The research involves investigation of automatic methods for image artifacts correction, tumor segmentation, and extraction of computerized features that help distinguish between benign and malignant lesions. Our hypothesis is that advanced methods for the computerized interpretation of state-of-the-art breast MRI will grant MRI a more leading role in diagnosis and monitoring of treatment for breast cancer, and greatly benefit breast cancer patients.

BODY

Training Accomplishments

At the time of this report, the recipient, Weijie Chen, of the Predoctoral Traineeship Award has taken 19 out of the 22 required courses towards the Ph.D. degree in medical physics. Two other courses are being taken in the current quarter. The courses include physics of medical imaging, physics of radiation therapy, mathematics for medical physicists, image processing, statistics, machine learning, numerical computation, topics in computer vision, anatomy of the body, radiation biology, and teaching assistant training.

Research Accomplishments

1. Database collection

The first part of our work has been collecting breast MR data. We have previously collected a database (referred to as **Database-I** in the following) containing images from 121 patients. Images were obtained using a T1-weighted 3D spoiled gradient echo sequence. After the acquisition of the precontrast series, Gd-DTPA contrast agent was injected intravenously by power injection with a dose of 0.2mmol/kg. Five postcontrast series were then taken with a time interval of 60 seconds. Each series contained 64 coronal slices with a matrix of 128 x 256 pixels and an in-plane resolution of $1.25 \times 1.25 mm^2$. Slice thickness ranged from 2 to 3 mm depending on breast size. For this database 121 primary mass lesions have been outlined by an experienced radiologist, 77 of the lesions are malignant and 44 lesions are benign, as revealed by biopsy.

We are also collecting more data in the University of Chicago Hospitals. The imaging technique is the same as Database-I above. We have collected 80 patients' images in the past year and more data are being collected currently.

2. Investigation of image features

We used Database-I for investigation of features that contribute to the diagnosis of breast cancer. The lesions were delineated by an experienced radiologist as well as independently by computer using an automatic volume-growing algorithm. Fourteen features that were extracted automatically from the lesions could be grouped into three categories based on: (I) morphology; (II) enhancement kinetics; and (III) time course of enhancement-variation over the lesion. A stepwise feature selection procedure was employed to select an effective subset of features, which were then combined by linear discriminant analysis (LDA) into a discriminant score, related to the likelihood of malignancy. The classification performances of individual features and the combined discriminant score were evaluated with receiver operating characteristic (ROC) analysis. With the radiologist-delineated lesion contours, stepwise feature selection yielded 4 features and an A_z value of 0.80 for the LDA in leave-one-out cross-validation testing. With the computer-segmented lesion volumes, it yielded 6 features and an A_z value of

0.86 for the LDA in the leave-one-out testing. A full description of this study is given in reference [5] which is attached as Appendix A.

3. Automatic identification of characteristic enhancement kinetics in breast MR lesions

In [5] we have demonstrated the usefulness of enhancement kinetics features in distinguishing between malignant and benign lesions. Due to uptake heterogeneity, however, the enhancement curve obtained from a specific region in the lesion may outperform that from averaging over the entire lesion. We have developed an automatic method, based fuzzy c-means (FCM) clustering analysis, to identify characteristic enhancement kinetics within the lesion. Our results have shown that the developed methods significantly improved the performance of enhancement kinetics in the diagnosis of breast cancer. A more detailed summary of these methods can be found in reference [6] which is also attached as Appendix B.

4. Development of methods for shading artifacts correction in breast MR images

Most clinical MR images are corrupted by shading artifacts, which is slow intensity variations of the same tissue over the image domain. Such artifacts might affect computerized analysis such as tissue segmentation. We developed a FCM based approach that simultaneously estimates the shading effect while segmenting the image. A full description of the methods is in reference [7] which is attached as Appendix C. Further study will be done to investigate the influence of the shading artifacts on lesion extent assessment and on the performance of features in the task of distinguishing between malignant and benign lesions.

5. Development of computerized methods for assessment of tumor extent

The assessment of tumor extent is a key step in computerized analysis of breast lesions, as the features are derived from the segmented lesion. In our previous study [5], we used a region-growing method for the segmentation of breast lesions. We developed a FCM based algorithm, which assesses the tumor extent based on analysis of the signal intensity-curves within a region of interest. The method has been shown to be more accurate than the region-growing method in the assessment of lesion extent using radiologist outlined lesion as a ground truth. This study will be presented at the 18th International Congress and Exhibition of Computer Assisted Radiology and Surgery, (CARS 2004), and the paper [8] has been accepted for publication in the Proceedings of CARS 2004. This short paper is attached in Appendix D.

KEY RESEARCH ACCOMPLISHMENTS

- Collection and maintenance of clinical database: dynamic MR images of over 200 patients have been collected which are well suitable for the proposed research;
- Investigation of lesion features: a new family of features have been investigated and proved to be useful in the diagnosis of breast cancer;
- Developed automatic methods for identification of characteristic enhancement kinetics in breast MR lesions which outperformed the performance of enhancement kinetics obtained from averaging over the entire lesion in the diagnosis of breast cancer;
- Developed automatic methods for shading artifacts correction in breast MR images which will potentially increase the accuracy of lesion segmentation and the performance of lesion features for diagnosis;
- Developed computerized methods for assessment of tumor extent which outperformed the previous region-growing method.

REPORTABLE OUTCOMES

Peer reviewed journal papers

- W. Chen, M. L. Giger, L. Lan, and U. Bick, "Computerized interpretation of breast MRI: Investigation of enhancement-variance dynamics," *Medical Physics*, 31(5):1076-1082, (2004).

Papers in conference proceedings

- W. Chen, M. L. Giger, and U. Bick, "Automated identification of temporal pattern with high initial enhancement in dynamic MR breast lesions using fuzzy c-means algorithm," *Proceedings SPIE*, 2004.
- W. Chen, M. L. Giger, "A fuzzy c-means (FCM) based algorithm for intensity inhomogeneity correction and segmentation of MR images," *Proceedings of IEEE International Symposium on Biomedical Imaging*, 2004.
- W.Chen, M.L.Giger, G. Newstead, U. Bick, L. Lan, "Computerized assessment of tumor extent in contrast-enhanced MR images of the breast," *Proceedings of 18th International Congress and Exhibition- Computer Assisted Radiology and Surgery, (CARS 2004), in press*

Presentations

- W. Chen, M. L. Giger, and U. Bick, "Automated identification of temporal pattern with high initial enhancement in dynamic MR breast lesions using fuzzy c-means algorithm," SPIE-Medical Imaging, San Diego, California, February 2004.

Posters

- W. Chen, M. L. Giger, "A fuzzy c-means (FCM) based algorithm for intensity inhomogeneity correction and segmentation of MR images," IEEE International Symposium on Biomedical Imaging, Arlington, Virginia, April 2004.
- W.Chen, M.L.Giger, G. Newstead, U. Bick, L. Lan, "Computerized assessment of tumor extent in contrast-enhanced MR images of the breast," 18th International Congress and Exhibition- Computer Assisted Radiology and Surgery (CARS 2004), Chicago, Illinois, June 2004.

Awards

- Doolittle-Harrison Fellowship ($500), The University of Chicago

CONCLUSIONS

The recipient of the Predoctoral Traineeship Award has taken all the required core courses and many research related elective courses as well. These trainings have proven useful for the recipient to achieve the proposed research goals.

During the first year, we have collected and maintained a dynamic breast MRI database that is well suitable for the proposed research on computerized interpretation of breast MR images. We have developed computerized methods for correction of shading artifacts, tumor segmentation, and feature extraction. The results have shown that computerized analysis and interpretation methods have great promise in increasing the objectivity, efficiency, and accuracy of the diagnosis of breast cancer.

Overall, we have well achieved the goals of the first year and laid a strong foundation for the research in the next two years. Our goals in the next two years include collection of more data, development of image registration methods for motion correction and assess the influence of motion artifacts in the diagnosis of breast cancer, investigation of features that would better distinguish between benign and malignant lesions, and evaluation of the overall systematic methods with an even larger database.

REFERENCES

[1] G.M. Newstead, "Role of MR in Breast Imaging," *RSNA Categorical Course in Breast Imaging*, 1999; pp287-293

[2] S.G. Orel and M.D. Schnall, "MR imaging of the breast for the detection, diagnosis, and staging of breast cancer," Radiology, 220:13-30 (2001)

[3] S.E. Harms, D.P. Flamig, "Breast MRI", Journal of clinical imaging, 25 (2001) 227-246

[4] C.K. Kuhl, and H.H. Schild, "Dynamic image interpretation of MRI of the breast," J. of Magn. Reson. Imaging, 12:965-974 (2000)

[5] W. Chen, M. L. Giger, L. Lan, and U. Bick, "Computerized interpretation of breast MRI: Investigation of enhancement-variance dynamics," *Medical Physics*, 31(5):1076-1082, (2004).

[6] W. Chen, M. L. Giger, and U. Bick, "Automated identification of temporal pattern with high initial enhancement in dynamic MR breast lesions using fuzzy c-means algorithm," *Proceedings SPIE*, 2004.

[7] W. Chen, M. L. Giger, "A fuzzy c-means (FCM) based algorithm for intensity inhomogeneity correction and segmentation of MR images," *Proceedings of IEEE International Symposium on Biomedical Imaging*, 2004.

[8] W.Chen, M.L.Giger, G. Newstead, U. Bick, L. Lan, "Computerized assessment of tumor extent in contrast-enhanced MR images of the breast," *Proceedings of 18th International Congress and Exhibition- Computer Assisted Radiology and Surgery, (CARS 2004), in press*

APPENDICS

Appendix A. Medical Physics Paper

Appendix B. SPIE Paper

Appendix C. IEEE-ISBI Paper

Appendix D. CARS 2004 Paper

Computerized interpretation of breast MRI: Investigation of enhancement-variance dynamics[a)]

Weijie Chen, Maryellen L. Giger,[b)] Li Lan, and Ulrich Bick
Department of Radiology, The University of Chicago, MC 2026, 5841 South Maryland Avenue, Chicago, Illinois 60637

(Received 23 July 2003; revised 12 February 2004; accepted for publication 13 February 2004; published 8 April 2004)

The advantages of breast MRI using contrast agent Gd-DTPA in the diagnosis of breast cancer have been well established. The variation of interpretation criteria and absence of interpretation guidelines, however, is a major obstacle for applications of MRI in the routine clinical practice of breast imaging. Our study aims to increase the objectivity and reproducibility of breast MRI interpretation by developing an automated interpretation approach for ultimate use in computer-aided diagnosis. The database in this study contains 121 cases: 77 malignant and 44 benign masses as revealed by biopsy. Images were obtained using a T1-weighted 3D spoiled gradient echo sequence. After the acquisition of the precontrast series, Gd-DTPA contrast agent was injected intravenously by power injection with a dose of 0.2 mmol/kg. Five postcontrast series were then taken with a time interval of 60 s. Each series contained 64 coronal slices with a matrix of 128×256 pixels and an in-plane resolution of 1.25×1.25 mm^2. Slice thickness ranged from 2 to 3 mm depending on breast size. The lesions were delineated by an experienced radiologist as well as independently by computer using an automatic volume-growing algorithm. Fourteen features that were extracted automatically from the lesions could be grouped into three categories based on (I) morphology, (II) enhancement kinetics, and (III) time course of enhancement-variation over the lesion. A stepwise feature selection procedure was employed to select an effective subset of features, which were then combined by linear discriminant analysis (LDA) into a discriminant score, related to the likelihood of malignancy. The classification performances of individual features and the combined discriminant score were evaluated with receiver operating characteristic (ROC) analysis. With the radiologist-delineated lesion contours, stepwise feature selection yielded four features and an A_z value of 0.80 for the LDA in leave-one-out cross-validation testing. With the computer-segmented lesion volumes, it yielded six features and an A_z value of 0.86 for the LDA in the leave-one-out testing. [DOI: 10.1118/1.1695652]

Key words: breast cancer, contrast-enhanced MRI, Gd-DTPA, computer-aided diagnosis (CAD), ROC analysis

I. INTRODUCTION

Breast MRI has emerged as a promising modality for the detection and diagnosis of breast cancer since the introduction of gadolinium-diethylenetriamine penta-acetic acid (Gd-DTPA) as a contrast agent.[1–3] Contrast-enhanced MRI (CE-MRI) allows lesions to be distinguished from normal tissues due to the increased vascularity and capillary permeability of tumors. CE-MRI offers three-dimensional spatial information and temporal information of breast cancer, qualifying it as an encouraging complementary modality to conventional imaging methods, such as x-ray mammography and sonography.

Despite its well-recognized advantages, applications of MRI in the routine clinical practice of breast imaging are limited. One of the most important obstacles is the lack of interpretation guidelines;[4,5] very few attempts have been made to standardize the interpretation of breast MR images. Among the few efforts in this regard is the work of the International Working Group on Breast MRI, which has developed and validated a detailed lexicon for breast MRI interpretation.[6] Investigators use a large variety of diagnostic criteria[2,3,7–13] that help classify lesions as benign or malignant. The interpretation criteria in the current literature fall into two major categories:[5,14] morphologic features[8,9,13] and enhancement kinetics,[2,3,12] i.e., the time course of signal intensity within the suspected lesions. While the studies using these criteria have shown promising results (sensitivity from 92% to 100%, specificity from 53% to 100%) as reported in a recent review,[15] significant variation does exist. The variation of the results may be due to two reasons from the interpretation aspect; one is the interobserver variation from different subjective judgments,[16–18] and the other is that the current interpretation schemes might not be sufficiently robust.

The aim of computerized interpretation of medical images is to obtain quantitative indices of malignancy. It has the advantage of being objective, automatic, and, furthermore, it may provide unique information that might be difficult to assess visually, especially for time-series 3D MR images.

This study aims to use computerized methods to investigate the potential of enhancement-variance dynamics in the interpretation of contrast-enhanced breast MR images. Auto-

matically extracted features are based on the time course of enhancement-variance within lesions. Features based on enhancement kinetics and morphology of lesions are studied as well for comparison. Also compared are the performances of features extracted from lesions delineated by experienced radiologist and those from lesions segmented by the computer using a volume-growing algorithm. Finally, different features are selected and merged into an estimate of malignancy using automated classification.

II. MATERIALS AND METHODS

A. Image database

The database in this study contains 121 cases: 77 malignant and 44 benign masses as revealed by biopsy. Images were obtained using a T1-weighted 3D spoiled gradient echo sequence (TR=8.1 ms, TE=4 ms, flip angle=30°). Fat suppression was not employed. The patients were scanned in prone position using a standard double breast coil on a 1.5 T whole-body MRI system (Siemens Vision, Siemens, Erlangen, Germany). After the acquisition of the precontrast series, Gd-DTPA contrast agent was delivered intravenously by power injection with a dose of 0.2 mmol/kg and a flow rate of 2 ml/s. Injection of contrast was followed by a saline flush of 20 ml with the same flow rate. Five postcontrast series were then taken with a time interval of 60 s. Each series contained 64 coronal slices with a matrix of 128 $\times$256 pixels and an in-plane resolution of 1.25$\times$1.25 mm^2. Slice thickness ranged from 2 to 3 mm depending on breast size. The image database had been retrospectively collected under an IRB-approved protocol.

B. Methods

The computerized interpretation scheme used in this study begins with the segmentation of the lesion within the image. The suspect masses were delineated both manually by an experienced radiologist (U.B.) and automatically by the computer using a 3D volume-growing algorithm.[19] Next, multiple features that characterize the spatial and kinetic properties of the lesions, and thus would potentially help differentiate the malignant cases from the benign cases, were extracted automatically. Stepwise feature selection[20] was employed to select a set of features that perform efficiently in classifying the lesions as malignant or benign. Using linear discriminant analysis[21] (LDA), the selected features were then merged into a single numerical value that is related to estimated likelihood of malignancy.

We evaluated the classification performance of individual features and the merged discriminant score in the task of distinguishing between malignant and benign lesions by using receiver operating characteristics (ROC) analysis.[22] The areaunder the maximum likelihood-fitted binormal ROC curve, A_z, was used as an index of performance.[23] We used the CLABROC[24,25] algorithm to determine the statistical significance (p value) of the difference between two A_z values, associated with two lesion delineation methods. The CLABROC algorithm uses a univariate z-score test to test the difference between areas under two ROC curves.

TABLE I. Features investigated in this study are grouped into three major categories.

I. Morphologic
$F_{I,1}$: Maximum std. of RGH value
$F_{I,2}$: Circularity
$F_{I,3}$: Irregularity
$F_{I,4}$: Margin gradient
$F_{I,5}$: Variance of margin gradient
II. Enhancement kinetics
$F_{II,1}$: Maximum uptake
$F_{II,2}$: Peak location
$F_{II,3}$: Uptake rate
$F_{II,4}$: Washout rate
III. Enhancement-variance dynamics
$F_{III,1}$: Maximum enhancement-variance
$F_{III,2}$: Peak location
$F_{III,3}$: Increasing rate
$F_{III,4}$: Decreasing rate
$F_{III,5}$: Enhancement-variance at time #1

1. Lesion delineation

For the manual delineation, a radiologist (U.B.), blinded to the histological diagnosis, contoured the enhanced tumor area in each slice that intersected the lesion in the subtraction images (postcontrast minus precontrast), using the nonsubtracted MR images as reference.

For the automatic segmentation by computer, we used a volume-growing based algorithm.[19] In this algorithm, the breast volume is first segmented at a threshold derived from the global histogram of voxel-values by maximizing the interclass variance between breast and background. Then the border of the segmented breast volume is removed by morphological erosion using a 3$\times$3$\times$3 structuring element. Next, regions with high contrast uptake are enhanced by voxelwise computation of the variance of the voxel values over time. A spherical region of interest (SROI) that encompasses the enhanced region is then automatically selected from a set of spheres expanding outwards from a manually selected seed point. From the preprocessed volume within the SROI, a segmentation threshold is then computed by maximizing the interclass variance between enhanced lesion and background voxels in the SROI. Finally, 6-point-connected volume growing is performed to yield the 3D segmented lesion.

2. Computerized feature extraction

In this study, our primary interest is to investigate the potential of enhancement variance dynamics features in the classification of suspicious lesions as malignant or benign. Other features are studied as well for comparison. Features investigated in this study, as listed in Table I, are grouped into three categories: (I) morphological features, (II) enhancement kinetics based features, and (III) features related to the time course of enhancement-variance over the lesion.

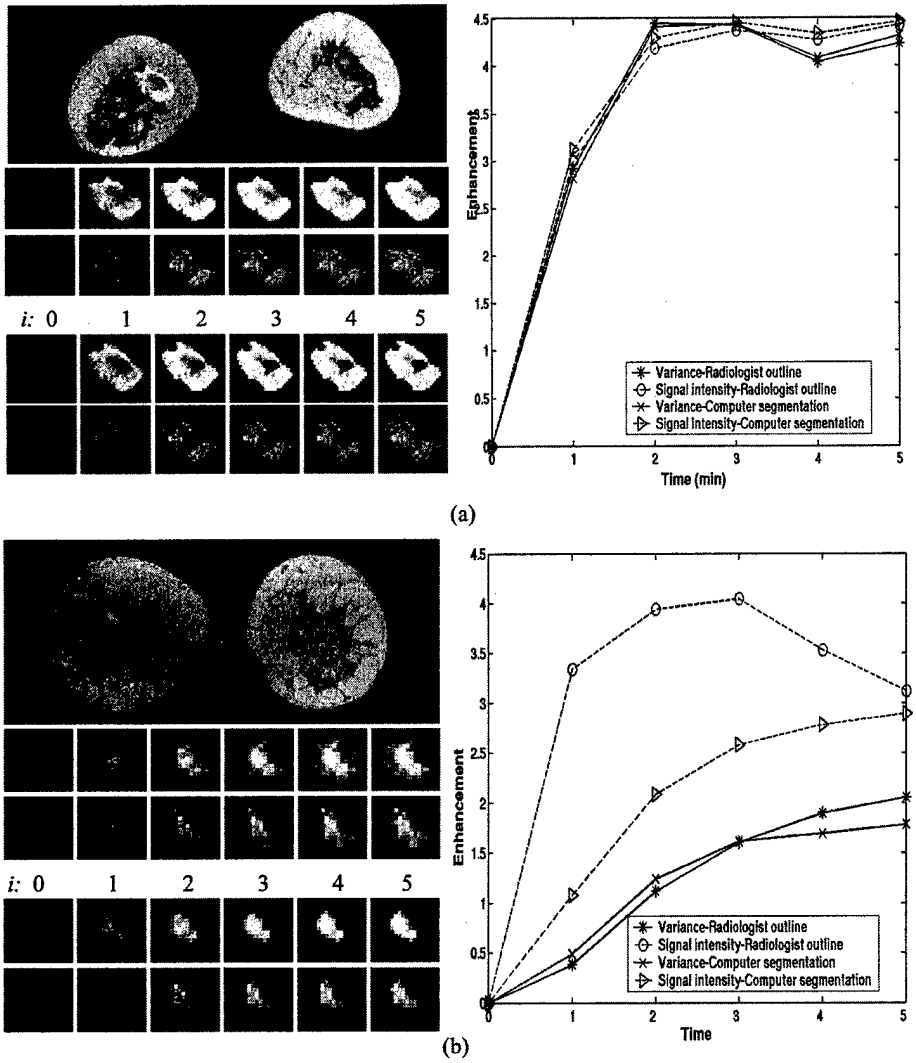

FIG. 1. Examples of lesion segmentation and the corresponding enhancement kinetics and enhancement-variance dynamics curves: (a) malignant case and (b) benign case. In each case, a central slice image of the volume lesion is shown (upper left). Also shown are the radiologist-outlined lesions and the corresponding lesion enhancement [Eq. (1)] at six time points (middle left), the computer-segmented lesion, and the corresponding lesion enhancement at six time points (lower left). The associated kinetics curves are shown (right).

The features in the first category have been described in detail in a previous paper from our group[12] and are only summarized here.

(i) Morphological features.[12] The feature "**maximum standard deviation (std) of radial gradient histogram (RGH)**" ($F_{I,1}$) quantifies how well the image structures in a suspected lesion extend in a spherical pattern originating from the center of the lesion. The feature "**circularity**" ($F_{I,2}$) measures conformity of a lesion to a spherical shape and the feature "**irregularity**" ($F_{I,3}$) indicates the roughness of the lesion surface. The features "**margin gradient**" ($F_{I,4}$) and "**variance of margin gradient**" ($F_{I,5}$) are related to the sharpness of the lesion margin by evaluating voxel-value gradients and their variations along the margin of the suspect lesion.

(ii) Enhancement kinetics based features. Enhancement kinetics is related to the time course of signal intensity within the lesion. Denote $S(\mathbf{r},i)$ as the voxel value at location $\mathbf{r}$ in the lesion at time frame i, i runs from 0 (i.e., the precontrast frame) to 5 (i.e., the last postcontrast frame). For each voxel in the lesion, the contrast enhancement is computed:

$$C(\mathbf{r},i)=\frac{S(\mathbf{r},i)-S(\mathbf{r},0)}{S(\mathbf{r},0)}, \quad i=0,1,...,5. \tag{1}$$

$C(\mathbf{r},i)$ is a quantity that has been shown[26] to be related to Gd-DTPA concentration in the extracellular space of breast tissue at voxel $\mathbf{r}$. In special circumstances this relation approaches linearity. Note that at $i=0, C(\mathbf{r},i)=0$. The enhancement dynamics can be described by the average enhancement over the lesion at each time point, i.e.,

$$\bar{C}(i)=\frac{1}{L}\sum_{r=1}^{L} C(\mathbf{r},i), \quad i=0,1,...,5, \tag{2}$$

where L is the number of voxels in the segmented lesion.

Four features are derived from the enhancement kinetics. The **maximum uptake** ($F_{II,1}$) is the maximum enhance-

ment, i.e., $F_{II,1}=\max_{i=0,1,...,5}\bar{C}(i)$. The time frame index at which the maximum enhancement occurs is a feature and is referred to here as "**peak location**" ($F_{II,2}$).

The **uptake rate** ($F_{II,3}$) of the contrast agent is defined as

$$F_{II,3}=F_{II,1}/F_{II,2}. \tag{3}$$

The **washout rate** ($F_{II,4}$) of the contrast agent is defined as

$$F_{II,4}=\begin{cases}\dfrac{F_{II,1}-\bar{C}(5)}{5-F_{II,2}} & (F_{II,2}\neq 5),\\ 0 & (F_{II,2}=5).\end{cases} \tag{4}$$

(iii) Enhancement-variance dynamics features. Enhancement-variance dynamics describes the time course of the spatial variance of the enhancement within the lesion and is defined by

$$V(i)=\frac{1}{L-1}\sum_{r=1}^{L}[C(\mathbf{r},i)-\bar{C}(i)]^2, \quad i=0,1,...,5. \tag{5}$$

Five features are derived from the enhancement-variance dynamics. The **maximum variation of enhancement** ($F_{III,1}$) is the maximum spatial variance of enhancement, i.e., $F_{III,1}=\max_{i=0,1,...,5}V(i)$. The time frame index at which the maximum variance occurs is a feature and is referred to here as "**peak location**" ($F_{III,2}$) of the enhancement-variance dynamics.

The **enhancement-variance increasing rate** ($F_{III,3}$) describes how fast the enhancement-variation within the lesion reaches maximum, defined by

$$F_{III,3}=F_{III,1}/F_{III,2}. \tag{6}$$

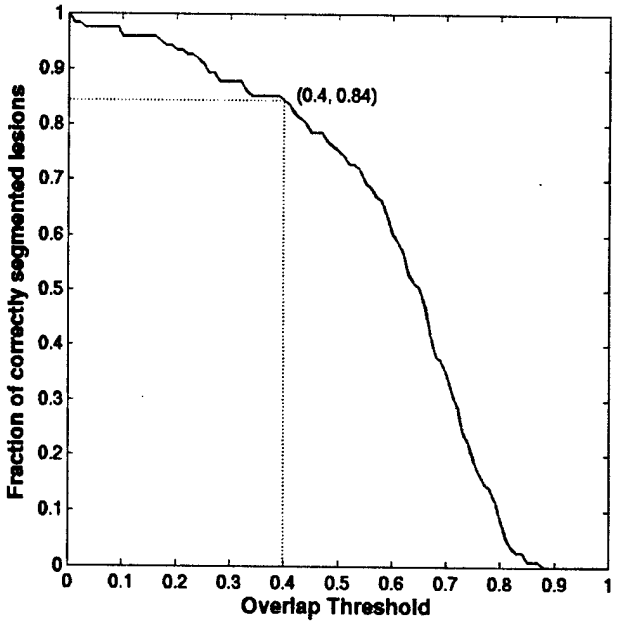

FIG. 2. Performance of the computer segmentation as compared to radiologist segmentation. Curve indicates the fraction of lesions correctly segmented as a function of the overlap criterion.

The **enhancement-variance decreasing rate** ($F_{III,4}$) indicates how fast the enhancement-variance decreases from the maximum, defined by

$$F_{III,4}=\begin{cases}\dfrac{F_{III,1}-V(5)}{5-F_{III,2}} & (F_{III,2}\neq 5),\\ 0 & (F_{III,2}=5).\end{cases} \tag{7}$$

TABLE II. Performance of 14 computer-extracted features in distinguishing between malignant and benign breast lesions that are delineated by both radiologist (column 2) and computer (column 3). The value after "±" is the standard deviation (s.d.) associated with each A_z value. The two tailed p-value was calculated using the univariate z-score test.

Feature	$A_z\pm 1$ s.d.: Radiologist outlined	$A_z\pm 1$ s.d: Computer segmented	p-value
I. Morphologic			
$F_{I,1}$: Maximum std. of RGH value	0.59±0.05	0.56±0.05	0.33
$F_{I,2}$: Circularity	0.57±0.06	0.65±0.05	0.42
$F_{I,3}$: Irregularity	0.66±0.05	0.54±0.06	0.19
$F_{I,4}$: Margin gradient	0.58±0.06	0.60±0.06	0.57
$F_{I,5}$: Variance of margin gradient	0.60±0.05	0.51±0.06	0.03
II. Enhancement kinetics			
$F_{II,1}$: Maximum uptake	0.55±0.06	0.51±0.06	0.25
$F_{II,2}$: Peak location	0.75±0.05	0.79±0.05	0.15
$F_{II,3}$: Uptake rate	0.68±0.05	0.66±0.05	0.50
$F_{II,4}$: Washout rate	0.73±0.05	0.78±0.05	0.09
III. Enhancement-variance dynamics			
$F_{III,1}$: Maximum variation of enhancement	0.50±0.06	0.52±0.06	0.86
$F_{III,2}$: Peak location	0.74±0.05	0.77±0.05	0.08
$F_{III,3}$: Increasing rate	0.58±0.06	0.58±0.06	0.96
$F_{III,4}$: Decreasing rate	0.74±0.05	0.73±0.05	0.90
$F_{III,5}$: Enhancement-variance at time #1	0.65±0.06	0.63±0.06	0.31

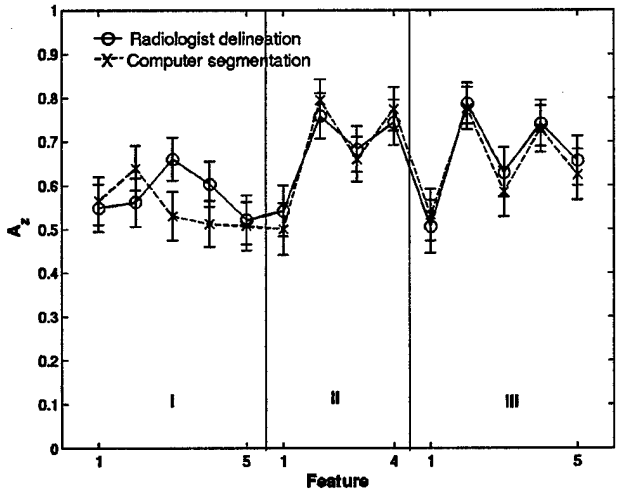

FIG. 3. Performance of the 14 computer-extracted features in distinguishing between malignant and benign breast lesions that are delineated by both radiologist (solid) and computer (dash).

The **enhancement-variance at the first postcontrast frame** ($F_{III,5}$), $V(1)$, reveals the uptake inhomogeneity at the early phase of uptake.

Figure 1 shows two examples (one malignant and one benign) of lesion segmentation and the corresponding enhancement kinetics curves and enhancement-variance curves. Note that the lesion sizes in the two examples are different, so in the figure the pixels of the smaller lesion [Fig. 1(b)] look larger.

III. RESULTS

Performance of the computer segmentation is shown in Fig. 2. Here overlap is defined as the volume of intersection of the radiologist-delineated lesion and the computer-segmented lesion divided by the volume of their union. In this database with 121 mass lesions, 84% of the lesions were correctly segmented at an overlap threshold of 0.4. The two segmentation examples shown in Fig. 1 had overlaps of (a) 0.77 and (b) 0.17, respectively.

Table II and Fig. 3 show the A_z values and the associated standard deviations indicating individual performance levels of the 14 features in the task of distinguishing between malignant and benign breast lesions that were delineated by either radiologist or computer. The results indicate that all three categories of features show potential for the classification task.

As also demonstrated in Table II and Fig. 3, at the significance level $p=0.05$, we failed to show a statistically significant difference between the performance (i.e., A_z) of features obtained using the radiologist-outlined lesions and the performance of those obtained with the computer-segmentation (except for feature $F_{I,5}$) in the task of distinguishing between malignant and benign breast lesions.

Stepwise feature selection[20] selected two sets of features—one set for each of the two methods of lesion delineation (Table III). The selected feature-set from features based on the radiologist-outlined lesions (set 1) includes four features: peak location of enhancement-variance dynamics ($F_{III,2}$), irregularity ($F_{I,3}$), washout rate of enhancement kinetics ($F_{II,4}$), and peak location of enhancement kinetics ($F_{II,2}$). The leave-one-out cross-validation using linear discriminant analysis to merge the selected features yields an A_z value of 0.80 in the task of distinguishing between malignant and benign lesions. The selected feature-set from features based on the computer-segmented lesions (set 2) includes six features: peak location of enhancement-variance dynamics ($F_{III,2}$), enhancement-variance increasing rate ($F_{III,3}$), peak location of enhancement kinetics ($F_{II,2}$), margin gradient ($F_{I,4}$), variance of margin gradient ($F_{I,5}$), and maximum standard deviation of RGH value ($F_{I,1}$). The leave-one-out cross-validation using linear discriminant analysis to merge the selected features yields an A_z value of 0.86.

IV. DISCUSSION

Enhancement kinetic analysis evaluates how the contrast enhancement within the lesion changes in a period of time, and reveals the uptake and washout characteristics of the intravenous contrast within a lesion. Studies have shown that malignant cases tend to have rapid uptake and washout.[12] Our results are consistent with such published results. In our analysis, 64% of the benign lesions showed no washout over the six acquisition frames, i.e., their enhancement-curves keep increasing. For malignant lesions only 24% demonstrated no washout. It is worth noting that all the features are calculated based on the average enhancement of the entire lesion. In clinical practice, however, radiologists can choose any region with which to assess the enhancement kinetics. Our future work of interest is to develop automatic methods to extract region of maximum enhancement. The enhancement-kinetics based features on such "hot areas" are expected to perform better in differential diagnosis.

Enhancement-variance dynamics reveals how the spatial distribution of contrast enhancement in the lesion region changes in a period of time. Our results showed that the spatial variance of enhancement peaks earlier in malignant lesions (Fig. 4). The enhancement-variance in a particular

TABLE III. Stepwise feature selection and the performance of the merged features using leave-one-out cross-validation. The value after "±" is the standard deviation (s.d.) associated with each A_z value. The two-tailed p-value was calculated using the univariate z-score test.

Radiologist outlined lesions		Computer segmented lesions		
Feature Set 1	$A_z \pm 1$ s.d.	Feature Set 2	$A_z \pm 1$ s.d.	p-value
$F_{III,2}F_{I,3}F_{II,4}F_{II,2}$	0.80±0.04	$F_{III,2}F_{III,3}F_{II,2}F_{I,4}F_{I,5}F_{I,1}$	0.86±0.04	0.07

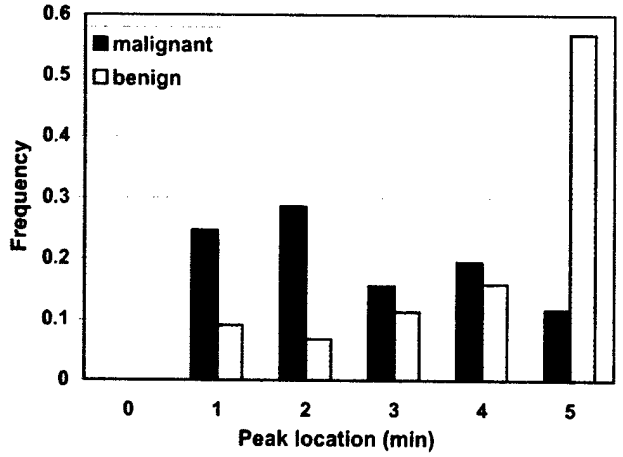

FIG. 4. Histogram of peak location of enhancement-variance dynamics for the computer-segmented lesions.

time frame reveals the degree of inhomogeneity of the enhancement. Our results show that malignant lesions tend to be less homogenous at the first postcontrast time frame ($F_{III,5}$). However, malignant and benign lesions showed similar results for the maximum inhomogeneity ($F_{III,1}$), as determined over all time frames.

The relative performance of the morphological and kinetic features depends on the MR imaging protocol involved. Basically, morphologic features perform better in high spatial resolution images and enhancement kinetics features perform better in high temporal resolution images.[27] Intuitively, morphological features might be more sensitive to lesion delineation methods. With the imaging protocol and lesion segmentation methods used in this study, overall, the kinetics features appeared to perform better than did the morphological features in the task of distinguishing between malignant and benign lesions.

At present, protocols used in breast MR imaging worldwide are far from reaching a consensus and optimal imaging parameters are still under investigation. The imaging technique used in our study is similar to that launched by Kaiser *et al.*,[2] which was called "the archetype of dynamic breast MRI" by Kuhl *et al.*:[5] acquisition of one precontrast and a series of postcontrast images including both breasts at a temporal resolution of 60 s. A potential limitation of the technique is that the data were acquired over only 5 min after contrast injection, as there is probably some useful information beyond 5 min.[28] The choice of the parameters is a tradeoff to allow for a shorter exam time, which is better accepted by patients and is less costly. This limited acquisition time problem might have some influence on the performance of washout related features ($F_{II,4}$,$F_{II,4}$). The influence on the performance of other temporal features should be much less severe as, in most cases, the signal reaches plateau within 5 min. We regard as an interesting research question the effect of acquisition time on the performance of computer-extracted features in distinguishing between malignant and benign lesions.

V. CONCLUSION

Our investigation with automated feature extraction and classification indicates that spatial-variance dynamics is a promising family of features in the task of distinguishing between malignant and benign MR breast lesions. Combining the morphological features of contrast enhancements, enhancement kinetics features, and the enhancement-variance dynamics features using computerized methods has the potential to complement the interpretation of radiologists in a consistent, objective, and accurate way.

ACKNOWLEDGMENTS

The research was supported in part by USPHS Grant No. CA89452 and DOD Breast Cancer Research Program DAMD 17-03-1-0245. MLG, LL, and UB are shareholders in R2 Technology, Sunnyvale, CA. It is the policy of the University of Chicago that investigators disclose publicly actual or potential significant financial interests that may appear to be affected by the research activities.

[a]Presented in part at the 2002 annual meeting of the AAPM, Montreal, Canada and the 2002 annual meeting of the RSNA, Chicago, IL.
[b]Author to whom correspondence should be addressed. Electronic mail: m-giger@uchicago.edu

[1] S. H. Heywang, D. Hahn, H. Schmidt, I. Krischke, W. Eiermann, R. Bassermann, and J. Lissner, "MR imaging of the breast using gadolinium-DTPA," J. Comput. Assist. Tomogr. **10**, 199–204 (1986).
[2] W. A. Kaiser and E. Zeitler, "MR imaging of the breast: fast imaging sequence with and without Gd-DTPA," Radiology **170**, 681–686 (1989).
[3] S. H. Heywang, A. Wolf, E. Pruss, T. Hilbertz, W. Eiermann, and W. Permanetter, "MR imaging of the breast with Gd-DTPA: use and limitations," Radiology **171**, 95–103 (1989).
[4] S. G. Orel and M. D. Schnall, "MR imaging of the breast for the detection, diagnosis, and staging of breast cancer," Radiology **220**, 13–30 (2001).
[5] C. K. Kuhl and H. H. Schild, "Dynamic image interpretation of MRI of the breast," J. Magn. Reson Imaging **12**, 965–974 (2000).
[6] D. M. Ikeda, N. M. Hylton, K. Kinkel, M. G. Hochman, C. K. Kuhl, W. A. Kaiser, J. C. Weinreb, S. F. Smazal, H. Degani, P. Viehweg, J. Barclay, and M. D. Schnall, "Development, standardization, and testing of a lexicon for reporting contrast-enhanced breast magnetic resonance imaging studies," J. Magn. Reson Imaging **13**, 889–895 (2001).
[7] S. G. Orel, M. D. Schnall, and C. M. Powell, "Staging of suspected breast cancer: effect of MR imaging and MR guided biopsy," Radiology **196**, 115–122 (1995).
[8] L. W. Nunes, M. D. Schnall, S. G. Orel, M. G. Hochman, C. P. Langlotz, C. A. Reynolds, and M. H. Torosian, "Breast MR imaging: interpretation model," Radiology **202**, 833–841 (1997).
[9] L. W. Nunes, M. D. Schnall, and S. G. Orel, "Update of breast MR imaging architectural interpretation model," Radiology **219**, 484–494 (2001).
[10] P. F. Liu, J. F. Debatin, R. F. Caduff, G. Kacl, E. Garzoli, and G. P. Krestin, "Improved diagnostic accuracy in dynamic contrast enhanced MRI of the breast by combined quantitative and qualitative analysis," Br. J. Radiol. **71**, 501–509 (1998).
[11] A. J. Bradley, B. M. Carrington, C. L. Hammond, R. Swindell, and B. Magee, "Accuracy of axillary MR imaging in treated breast cancer for distinguishing between recurrent tumor and treatment effects: does intravenous Gd-DTPA enhancement help in cases of diagnostic dilemma," Clin. Radiol. **55**, 921–928 (2000).
[12] C. K. Kuhl, P. Mielcareck, S. Klaschik, C. Leutner, E. Wardelmann, J. Gieseke, and H. H. Schild, "Dynamic breast MR imaging: Are signal intensity time course data useful for differential diagnosis of enhancing lesion?," Radiology **211**, 101–110 (1999).
[13] K. G. A. Gilhuijs, M. L. Giger, and U. Bick, "Computerized analysis of breast lesions in three dimensions using dynamic magnetic-resonance imaging," Med. Phys. **25**, 1647–1654 (1998).

[14] E. A. Morris, "Breast cancer imaging with MRI," Radiol. Clin. North Am. **40**, 443–466 (2002).
[15] P. J. Kneeshaw, L. W. Turnbull, and P. J. Drew, "Current applications and future direction of MR mammography," Br. J. Cancer **88**, 4–10 (2003).
[16] K. Kinkel, T. H. Helbich, L. J. Esserman, J. Barclay, E. H. Schwerin, E. A. Sickles, and N. M. Hylton, "Dynamic high-spatial-resolution MR imaging of suspicious breast lesions: Disgnostic criteria and interobserver variability," AJR, Am. J. Roentgenol. **175**, 35–43 (2000).
[17] S. J. Kim, E. A. Morris, L. Liberman, D. J. Ballon, L. R. L. Trenta, O. Hadar, A. Abramson, and D. D. Dershaw, "Observer variability and applicability of BI-RADS terminology for breast MR imaging: Invasive carcinomas as focal masses," AJR, Am. J. Roentgenol. **177**, 551–557 (2001).
[18] U. Wedegärtner, U. Bick, K. Wörtler, E. Rummeny, and G. Bongartz, "Differentiation between benign and malignant findings on MR-mammography: usefulness of morphological criteria," Eur. Radiol. **11**, 1645–1650 (2001).
[19] K. G. A. Gihuijs, M. L. Giger, and U. Bick, "A method for computerized assessment of tumor extent in contrast-enhanced MR images of the breast," in *Computer-Aided Diagnosis in Medical Imaging*, edited by K. Doi, H. MacMahon, M. L. Giger, and K. R. Hoffmann (Elsevier, Amsterdam, 1999), pp. 305–310.
[20] J. Neter, W. Wasserman, and M. H. Kutner, *Applied Linear Statistical Models Regression, Analysis of Variance, and Experimental Designs*, 2nd ed. (Irwin, Homewood, 1985).
[21] R. A. Johnson and D. W. Wichern, *Applied Multivariate Statistical Analysis*, 3rd ed. (Prentice–Hall, Englewood Cliffs, NJ, 1992).
[22] C. E. Metz, "Some practical issues of experimental design and data analysis in radiological ROC studies," Invest. Radiol. **24**, 234–245 (1989).
[23] Y. Jiang, C. E. Metz, and R. M. Nishikawa, "A receiver operating characteristic partial area index for highly sensitive diagnostic tests," Radiology **201**, 745–750 (1996).
[24] C. E. Metz, P-L. Wang, and H. B. Kronman, "A new approach for testing the significance of differences between ROC curves measured from correlated data," in *Information Processing in Medical Imaging*, edited by Deconinck (Nijhoff, The Hague, The Netherlands, 1984), pp. 432–435.
[25] C. E. Metz, B. A. Herman, and C. A. Roe, "Statistical comparison of two ROC-curve estimates obtained from partially-paired datasets," Med. Decision Making **18**, 110–121 (1998).
[26] U. Hoffmann, G. Brix, M. V. Knopp, T. Heb, and W. J. Lorenz, "Pharmacokinetic mapping of the breast: A new method for dynamic MR mammography," Magn. Reson. Med. **33**, 506–514 (1995).
[27] J. C. Weinreb and G. Newstead, "MR imaging of the breast," Radiology **196**, 593–610 (1995).
[28] H. Sherif, A. E. Mahfouz, H. Oellinger, J. Hadijuana, J. U. Blohmer, M. Taupitz, R. Felix, and B. Hamm, "Peripheral washout sign on contrast-enhanced MR images of the breast," Radiology **205**, 209–213 (1997).

Automated identification of temporal pattern with high initial enhancement in dynamic MR lesions using fuzzy c-means algorithm

Weijie Chen, Maryellen L. Giger*, Ulrich Bick

Department of Radiology, The University of Chicago,Chicago, IL USA 60637

ABSTRACT

In contrast-enhanced (CE) MRI of the breast, signal-intensity time curves have been proven useful in differentiating between benign and malignant lesions. Due to uptake heterogeneity in the breast lesion, however, the signal-intensity time curve obtained from a specific region in the lesion may outperform that from the entire lesion. In this study, we propose the use of fuzzy c-means (FCM) clustering algorithms to reveal different temporal patterns within the breast lesion. The algorithm finds fuzzy cluster centers (i.e., temporal patterns) and assigns membership values to each voxel. The temporal pattern with maximum initial enhancement is selected as the representative curve of the lesion and the thresholded membership map is the identified region of fast enhancement. The approach was applied to the analysis of 121 lesions (77 malignant and 44 benign). The resulting representative curves were classified with linear discriminant analysis (LDA). The differentiation performance of LDA output in leave-one-out cross evaluation was assessed using receiver operating characteristic (ROC) analysis. Our results show that the use of FCM significantly improved the performance of signal-intensity time curves in the task of distinguishing between malignant and benign lesions.

Keywords: Fuzzy c-means, breast cancer, contrast-enhanced MRI, tumor heterogeneity, computer-aided diagnosis (CAD)

1. INTRODUCTION

Breast cancer is the most common cancer and the second leading cause of cancer death among women in the Western countries. Mammography is currently the primary imaging modality in diagnostic and screening practice and has achieved significant success, though there is considerable limitations: $8-25\%$ of cancers are missed and $70-80\%$ of biopsies turn out to be benign. Contrast-enhanced magnetic resonance imaging (CE-MRI) using Gd-DTPA is a promising complementary modality in breast imaging[1,2,3] and has become more widely used recently as a supplemental imaging technique,[4] particularly in the radiographically dense breast. CE-MRI offers three-dimensional spatial information and temporal information, and has demonstrated extremely high sensitivity for breast cancer. The specificity of CE-MRI, however, is low and this fact has led intense efforts to investigate distinguishing characteristics between malignant and benign lesions.[5,6,7,8,9,10]

In CE-MRI of the breast, signal-intensity time curves have been proven useful in differentiating between benign and malignant lesions.[8,9] Due to uptake heterogeneity in the breast lesion, however, the signal-intensity time curve obtained from a specific region in the lesion may outperform that from the entire lesion. In this study, we propose the use of fuzzy c-means (FCM) clusterings algorithm to reveal different temporal patterns within the breast lesion.

*Send correspondence to M.L.G., E-mail: m-giger@uchicago.edu; Phone: +1 (773) 834-5099; Fax: +1 (773) 702-0371

2. MATERIALS AND METHODS

2.1. Database

Our database in this study contains 121 cases: 77 malignant and 44 benign masses as determined by biopsy. Images were obtained using a T1-weighted 3D spoiled gradient echo sequence ($TR = 8.1\,ms$, $TE = 4\,ms$, $flip\,angle = 30^0$). Fat suppression was not employed. The patients were scanned in prone position using a standard double breast coil on a $1.5\,T$ whole-body MRI system (Siemens Vision, Siemens, Erlangen, Germany). After the acquisition of the precontrast series, Gd-DTPA contrast agent was delivered intravenously by power injection with a dose of $0.2\,mmol/kg$ and a flow rate of $2\,ml/s$. Injection of contrast was followed by a saline flush of $20\,ml$ with the same flow rate. Five postcontrast series were then taken with a time interval of 60 *seconds*. Each series contained 64 coronal slices with a matrix of 128×256 pixels and an in-plane resolution of $1.25 \times 1.25\,mm^2$. Slice thickness ranged from 2 to $3\,mm$ depending on breast size. The image database had been retrospectively collected under an IRB-approved protocol.

2.2. Tumor segmentation

The mass lesions were manually delineated in each slice by an experienced radiologist (U.B.). The manual segmentation was performed in the subtraction images (postcontrast−precontrast) in which the tumor areas were enhanced in each slice. All five subtraction images were used for this purpose. In addition, the precontrast images were used as reference, and complementary information from other imaging modalities were used as well.

2.3. Fuzzy c-means clustering analysis

Our aim is to identify different temporal patterns of all the voxels within the lesion using FCM algorithm. In this context, the standard FCM algorithm[11] is an optimization problem for partitioning a lesion of N voxels, $X = \{\mathbf{x_i}\}_{i=1}^{N}$ ($\mathbf{x_i} = \{x_{i0}, x_{i1}, ..., x_{i5}\}$), into c classes (temporal patterns).

$$arg \min_{U,V} \quad \{J(U,V;X) = \sum_{k=1}^{c}\sum_{i=1}^{N} u_{ki}^{p} \|\mathbf{x_i} - \mathbf{v_k}\|^2\} \tag{1}$$

subject to:

$$\sum_{k=1}^{c} u_{ki} = 1 \quad \forall i$$

$$0 \le u_{ki} \le 1 \quad \forall k, i$$

where U is the *partition matrix* whose element u_{ki} is the *membership* of the ith voxel for kth class. V is the *centroid matrix* whose kth row $\mathbf{v_k} = \{v_{k0}, v_{k1}, ..., v_{k5}\}$ is the centroid vector of kth class, i.e., the temporal pattern prototype of kth class. The parameter p, called *fuzzy index*, is a weighting exponent on each fuzzy membership and determines the amount of "fuzziness" of the resulting partition. The norm operator $\|\cdot\|$ represents the standard Euclidean distance. The objective function J is minimized when high membership values are assigned to the voxels whose intensities are close to the centroid of its particular class, and low membership values are assigned to the voxels whose intensities are far from the centroid.

To solve (1), we take the first derivatives of J with respect to $u_{ki}, \mathbf{v_k}$ and set them equal to zero. We thus obtain two necessary conditions for J to be at a minimum:

$$u_{ki} = \frac{1}{\sum_{l=1}^{c} (\frac{\|\mathbf{x_i} - \mathbf{v_k}\|}{\|\mathbf{x_i} - \mathbf{v_l}\|})^{2/(p-1)}} \tag{2}$$

$$\mathbf{v_k} = \frac{\sum_{i=1}^{N} u_{ki}^{p} \mathbf{x_i}}{\sum_{i=1}^{N} u_{ki}^{p}} \tag{3}$$

In implementation, matrix V is randomly initialized,then U and V are obtained through an iterative process using (2) and (3). The stopping criteria of the iteration is that the (Euclidean) distance between the current

centroids and the centroids in the previous iteration is less than a user specified small number,i.e., $\|V_{new} - V_{old}\| < \epsilon$. After we get V,i.e., c temporal patterns, we select the temporal pattern with maximum initial enhancement as the representative curve of the lesion. The corresponding membership map, after thresholded, is the identified region of fast enhancement.

2.4. Evaluation

We compared the signal-intensity curve obtained from FCM with that from averaging the signal intensities over the entire lesion. We extracted four features from each curve, which was represented by 6 time points, i.e., $\{s_0, s_1, ..., s_5\}$, where $s_i (i = 0, 1, ..., 5)$ is the signal intensity at time point i. Denoting s^* as the maximum of the six signal intensities and p the time point of s^*,the four features are defined as:

$$maximum\ uptake = (s^* - s_0)/s_0$$

$$peak\ location = p$$

$$uptake\ rate = (s^* - s_0)/(s_0 \times p)$$

$$washout\ rate = \begin{cases} \frac{s^* - s_5}{s_0 \times (5-p)} & \text{if } p \neq 5 \\ 0 & \text{if } p = 5 \end{cases}$$

We used linear discriminant analysis (LDA)[12] to combine the four features in the task of distinguishing between malignant and benign lesions. The differentiation performance of the LDA output in leave-one-out cross evaluation was assessed using receiver operating characteristic (ROC) analysis.[13,14]

3. RESULTS

Figure 1 shows a malignant case with a breast lesion displayed across 6 slices. The membership map displayed was thresholded at 0.4, i.e., the labeled voxels have membership values over 0.4 to the cluster represented by the solid curve in Figure 1. The signal intensity time curve averaged over the entire lesion (dashed curve) shows a "plateau" pattern. The FCM generated curve, with high initial enhancement, (solid curve) shows a "washout" pattern that is characteristic of malignant lesions.

The four features from signal-intensity time curve obtained from FCM yielded an A_z value of 0.80, whereas the features from the signal-intensity time curve obtained over the entire lesion yielded an A_z value of 0.68 ($p\ value = 0.007$).

4. SUMMARY

Currently radiologists manually select a region within a lesion using parametric images. We explored an unsupervised learning algorithm, which is data-driven and non-parametric, with which to analyze the heterogeneity of Gd-DTPA uptake in breast lesions and to automatically identify the high-initial-enhancement regions. The algorithm has the advantage of being automatic, fast, and efficient.

The proposed FCM-based algorithm is useful in automatically identifying the temporal pattern with high initial enhancement in CE-MRI of breast lesions and improves the differentiation performance of enhancement kinetics.

ACKNOWLEDGMENTS

The research was supported in part by DOD Breast Cancer Research Program DAMD17-03-1-0245 and USPHS grant CA89452. M. L. Giger and U. Bick are shareholders in R2 Technology, Sunnyvale, CA. It is the policy of the University of Chicago that investigators disclose publicly actual or potential significant financial interests that may appear to be affected by the research activities.

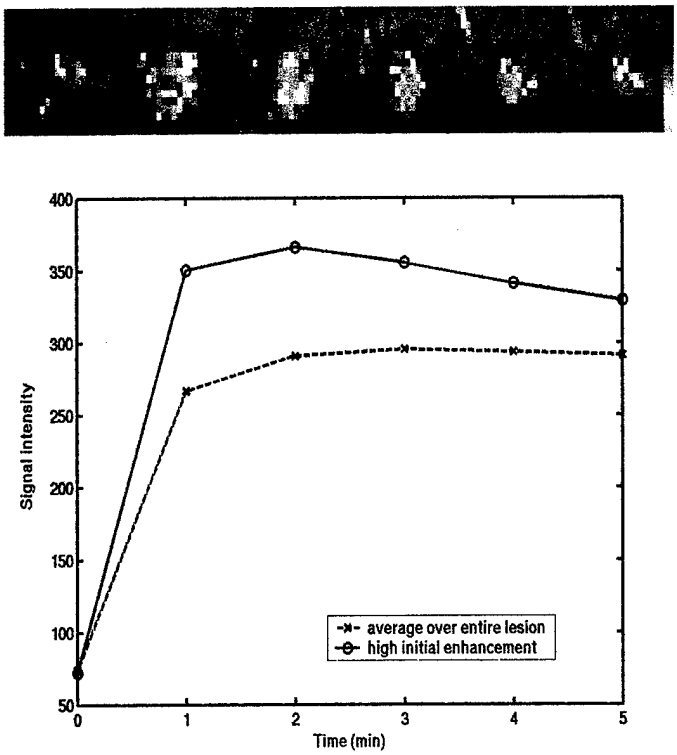

Figure 1. A malignant case with a 3-D lesion displayed across 6 slices. The membership map displayed was thresholded at 0.4, i.e., the color-labeled voxels have membership values over 0.4 to the cluster belonging to the solid curve. The signal intensity time curve averaged over the entire lesion (dashed curve) shows a "plateau" pattern. The FCM curve, with high initial enhancement, (solid curve) shows a "washout" pattern that is characteristic of malignant lesions.

REFERENCES

1. S. H. Heywang, D. Hahn, H. Schmidt, I. Krischke, W. Eiermann, R. Bassermann, and J. Lissner, "MR imaging of the breast using gadolinium-DTPA," *J Comput Assist Tomogr*, 10, 199-204 (1986)
2. W. A. Kaiser, E. Zeitler, "MR imaging of the breast: fast imaging sequence with and without Gd-DTPA," *Radiology*, 170, 681-686 (1989)
3. J. C. Weinreb, G. Newstead,"MR imaging of the breast,"
4. M. D. Schnall, "Breast MR imaging", *Radiol Clin N Am*, 41:43-50 (2003) *Radiology*,196(3), pp. 593-610, Sept. 1995.
5. L. W. Nunes, M. D. Schnall, S. G. Orel, M. G. Hochman, C. P. Langlotz, C. A. Reynolds and M. H. Torosian, "Breast MR imaging: interpretation model," *Radiology*, 202, 833-841 (1997)
6. L. W. Nunes, M. D. Schnall, and S. G. Orel, "Update of Breast MR Imaging Architectural Interpretation Model," *Radiology*, 219, 484 - 494 (2001)
7. K. G. A. Gilhuijs, M. L. Giger and U. Bick, "Computerized analysis of breast lesions in three dimensions using dynamic magnetic-resonance imaging," *Med. Phys.* 25, 1647-1654 (1998)
8. P. F. Liu, J. F. Debatin, R. F. Caduff, G. Kacl, E. Garzoli, G. P. Krestin, "Improved diagnostic accuracy in dynamic contrast enhanced MRI of the breast by combined quantitative and qualitative analysis," *Br J Radiol* 71, 501-509 (1998)
9. C. K. Kuhl, P. Mielcareck, S. Klaschik, et al, "Dynamic Breast MR Imaging: Are Signal Intensity Time Course Data Useful for Differential Diagnosis of Enhancing Lesion?" *Radiology*, 211, 101-110 (1999)
10. W. Chen, M. L. Giger, L. Lan, U. Bick,"Computerized interpretation of breast MRI: Investigation of enhancement-variance dynamics," *Med. Phys.,in press.*
11. J. Bezdek, L. Hall, and L. Clarke, "Review of MR image segmentation using pattern recognition," *Med. Phys.*, vol. 20, pp. 1033-1048 (1993)
12. R. A. Johnson and D. W. Wichern, *Applied Multivariate Statistical Analysis*, 3rd ed. (Prentice-Hall, Englewood Cliffs, New Jersey, 1992).
13. C. E. Metz, "Some practical issues of experimental design and data analysis in radiological ROC studies," *Invest. Radiol.* 24, 234-245 (1989)
14. C. E. Metz, B. A. Herman, and C. A. Roe, "Statistical comparison of two ROC-curve estimates obtained from partially-paired datasets," *Medical Decision Making* 18, 110-121 (1998)

A fuzzy c-means (FCM) based algorithm for intensity inhomogeneity correction and segmentation of MR images

Weijie Chen
Dept. of Radiology
The University of Chicago
Chicago,IL 60637
Email: weijie@uchicago.edu

Maryellen L. Giger
Dept. of Radiology
The University of Chicago
Chicago,IL 60637
Email: m-giger@uchicago.edu

Abstract— **Magnetic resonance images are often corrupted by intensity inhomogeneity, which manifests itself as slow intensity variations of the same tissue over the image domain. Such shading artifacts must be corrected before doing computerized analysis such as intensity-based segmentation and quantitative analysis. In this paper, we present a fuzzy c-means (FCM) based algorithm that simultaneously estimates the shading effect while segmenting the image. A multiplier field term that models the intensity variation is incorporated into the FCM objective function which is minimized iteratively. In each iteration, the bias field is estimated based on the current tissue class centroids and the membership values of the voxels and then smoothed by an iterative low-pass filter. The efficacy of the algorithm is demonstrated on clinical breast MR images.**

I. Introduction

Magnetic resonance imaging (MRI) has many advantages over other diagnostic imaging modalities, such as high contrast between soft tissues, high spatial resolution and inherent 3D nature, thus has gained wide clinical applications. Breast MRI, for example, has been widely investigated in the past decade in the detection and diagnosis of breast cancer as a complementary modality to X-ray mammography[1], in assessment of the localization and extent of breast lesions[2], and in monitoring tumor response to therapy[3]. Furthermore, breast MRI can be used for quantitative assessment of fibroglandular tissue percentage[4] which is a predictor of breast cancer risk. While qualitative visual assessment is often used by radiologists in a clinical environment, computerized quantitative analysis is increasingly needed to aid the radiologists increase both the accuracy and the efficiency of the diagnosis.

Magnetic resonance images are often corrupted by intensity inhomogeneity, which manifests itself as slow intensity variations of the same tissue over the image domain[5]. Such shading artifacts is the major source of difficulty for computerized analysis such as intensity-based segmentation and quantitative analysis. A number of algorithms have been proposed for the correction of spatial intensity inhomogeneity. Wells *et al.*[6], Guillemaud and Brady[7] developed a statistical approach based on the expectation-maximization (EM) algorithm that simultaneously estimates the bias field and segments the image into different tissue classes. Their methods yielded impressive results on brain MR images but has the disadvantage of being computationally intensive and requiring prior knowledge on intensity distributions of different tissue classes. Pham and Prince[8] proposed an adaptive fuzzy c-means (AFCM) algorithm for fuzzy segmentation of images while compensating for intensity inhomogeneities. AFCM is robust in convergence because the objective function to be minimized has regularization terms that ensure the estimated bias field is smooth and slowly varying. Ahmed *et al.*[9] proposed a bias-correction fuzzy c-means (BCFCM) algorithm in which they incorporated a neighborhood regularizer into the FCM objective function to allow labeling of a voxel to be influenced by the labels in its immediate neighborhood, making the algorithm insensitive to salt and peppernoise. However, they failed to address that the algorithm may converge to unwanted results without any constraint on the bias field. Li *et al.*[10] combined the AFCM and the neighborhood regularizer in BCFCM and obtained promising results in images with high noise level. The AFCM based methods, however, are computationally intensive and faster algorithm is needed in real-time clinical applications.

In this paper, we present a fast fuzzy c-means (FCM) based algorithm that simultaneously estimates the bias field while segmenting the image. A multiplier field term that models the intensity variation is incorporated into the FCM objective function which is minimized iteratively. In each iteration, the bias field is estimated based on the current tissue class centroids and the membership values of the voxels and then smoothed by an iterative low-pass filter. The efficacy of the algorithm is demonstrated on clinical breast MR images.

II. Methods

A. Bias field model

The observed MRI signal intensity is modeled as the "true" signal intensity multiplied by a spatially-varying factor called *gain* field, namely,

$$Y_i = X_i G_i \qquad \forall \quad i \in \{1, 2, \ldots, N\} \tag{1}$$

where Y_i, X_i, and G_i are the observed intensity, true intensity, and *gain* field at the ith voxel, respectively. N is the total number of voxels in the MR image. The artifact can be modeled as an additive *bias* field by applying a logarithmic transformation to both sides of (1)[6]

$$y_i = x_i + \beta_i \qquad \forall \quad i \in \{1, 2, \ldots, N\} \tag{2}$$

where y_i, x_i are the observed and true log-transformed intensities at the ith voxel, respectively, and β_i is the bias field at the ith voxel. By incorporating the bias field model into a fuzzy c-mean framework, we will be able to iteratively estimate both the true intensity and the bias field from the observed intensity.

B. Algorithm

In the image segmentation context, the standard FCM algorithm[11] is an optimization problem for partitioning an image of N voxels, $X = \{x_i\}_{i=1}^N$, into c (tissue) classes

$$\min_{U,V} \quad \{J(U, V; X) = \sum_{k=1}^{c} \sum_{i=1}^{N} u_{ki}^p \|x_i - v_k\|^2\} \tag{3}$$

subject to:

$$\sum_{k=1}^{c} u_{ki} = 1 \quad \forall i$$

$$0 \leq u_{ki} \leq 1 \quad \forall k, i$$

where U is the *partition matrix* whose element u_{ki} is the *membership* of the ith voxel for kth class. V is the *centroid* vector whose element v_k is the centroid (or prototype) of kth class. The parameter p, called *fuzzy index*, is a weighting exponent on each fuzzy membership and determines the amount of "fuziness" of the resulting partition. The norm operator $\|\cdot\|$ represents the standard Euclidean distance. The objective function J is minimized when high membership values are assigned to the pixels whose intensities are close to the centroid of its particular class, and low membership values are assigned to the voxels whose intensities are far from the centroid.

To incorporate the bias field into the FCM framework, we substitute (2) into (3). Then the fuzzy segmentation with the presence of bias field becomes a constrained optimization problem

$$\min_{U,V,B} \quad \{J_b(U, V, B; Y) = \sum_{k=1}^{c} \sum_{i=1}^{N} u_{ki}^p \|y_i - \beta_i - v_k\|^2\} \tag{4}$$

subject to:

$$\sum_{k=1}^{c} u_{ki} = 1 \quad \forall i$$

$$0 \leq u_{ki} \leq 1 \quad \forall k, i$$

where $Y = \{y_i\}_{i=1}^N$ is the observed image, $B = \{\beta_i\}_{i=1}^N$ is the bias field image.

To solve (4), we take the first derivatives of J_b with respect to u_{ki}, v_k, and β_k and setting them equal to zero. We thus obtain three necessary conditions for J_b to be at a minimum.

$$u_{ki}^* = \frac{1}{\sum_{l=1}^{c} \left(\frac{\|y_i - \beta_i - v_k\|}{\|y_i - \beta_i - v_l\|}\right)^{2/(p-1)}} \tag{5}$$

$$v_k^* = \frac{\sum_{i=1}^{N} u_{ki}^p (y_i - \beta_i)}{\sum_{i=1}^{N} u_{ki}^p} \tag{6}$$

$$\beta_i^* = y_i - \frac{\sum_{k=1}^{c} u_{ki}^p v_k}{\sum_{k=1}^{c} u_{ki}^p} \tag{7}$$

From the first eye, an iterative scheme for minimizing the objective function J_b is straightforward by performing Picard iteration through the above three necessary conditions for (4) to be minimized. This is not the whole story, however, because B obtained from (7) is a "residual" image but not necessarily be the bias field image. A residual image could always be found that would set J_b to zero. Pham and Prince's AFCM algorithm solved the problem by introducing regularization terms into the objective function that ensure the resulted bias field image being smooth. The regularization terms, however, make the estimation of the bias field a computationally intensive process. Another solution is that we estimate the bias field by filtering the residual image B in (7) using an iterative low-pass spatial filter. This filtering strategy is based on the fact that the bias field is of low spatial frequency and the assumption that other components in the residual image is of higher frequency. The steps for our algorithm can then be described as the following:

1) Initialize class centroid values, $\{v_k\}_{k=1}^c$. Initialize $\{\beta_i\}_{i=1}^N$ with zeros.
2) Update partition matrix U using (5).
3) Update class centroids V using (6).
4) Estimate residual image using (7).
5) Filter the residual image using an iterative low-pass filter.
6) Go to Step 2 unless the following termination criterion is satisfied:

$$\|V_{new} - V_{old}\| < \epsilon \tag{8}$$

where ϵ is a user-chosen threshold.

III. Results

In this section we demonstrate the efficacy of our algorithm by applying it to clinical breast MR images. The images were obtained using a General Electric Signa 1.5-Tesla clinical MR scanner. We set the parameter *fuzzy index* $p = 2$, the termination criterion $\epsilon = 0.001$. The images were thresholded before analysis so that only tissues of interest were included in the computation and the background was excluded. We set the number of classes $c = 2$.

Fig.1(a) shows a clinical MR image corrupted by intensity inhomogeneity. Fig. 1(b) shows the estimated bias field using our algorithm and Fig.1(c) shows the corrected image using the bias field in (b). The membership map for dense tissue class is shown in Fig.1(d). Applying standard FCM algorithm

(a)

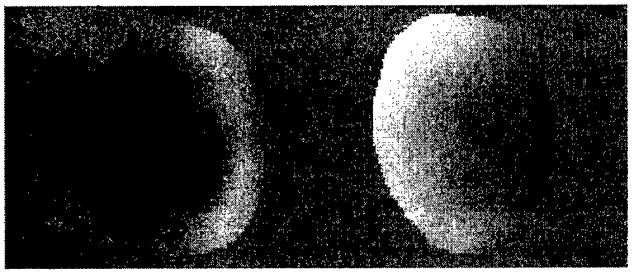

(b)

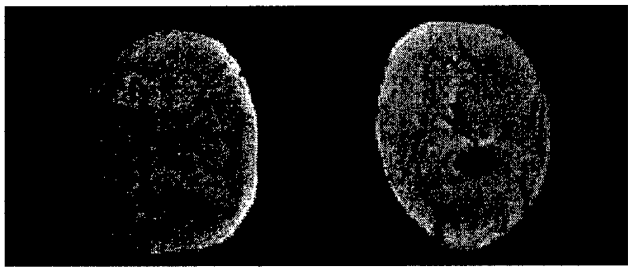

(c)

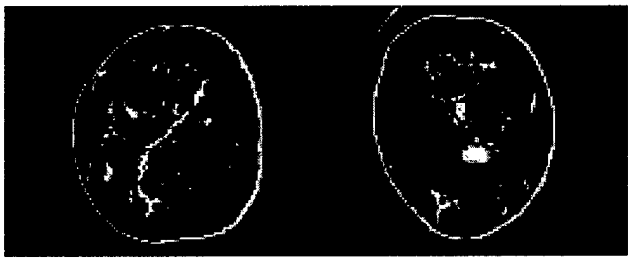

(d)

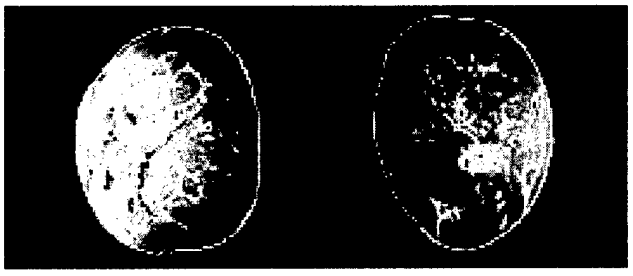

(e)

Fig. 1. Application of the proposed algorithm to a clinical breast MR image: (a)The original image. (b) Estimated bias field. (c) Corrected image. (d) The membership map for the dense-tissue class. (e) For comparison, the membership mapping from the standard FCM algorithm.

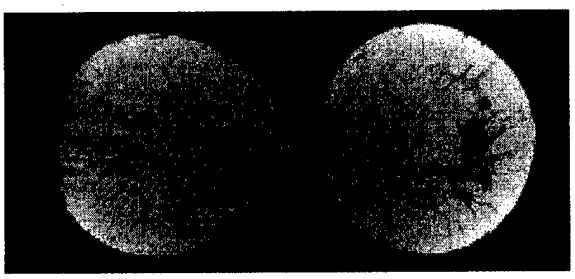

(a)

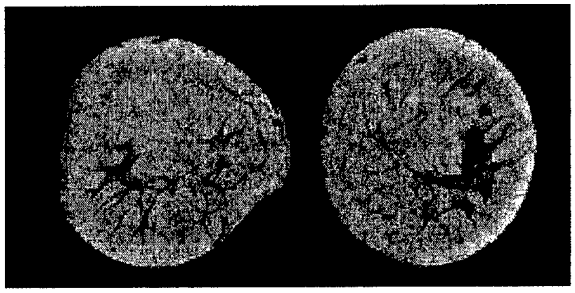

(b)

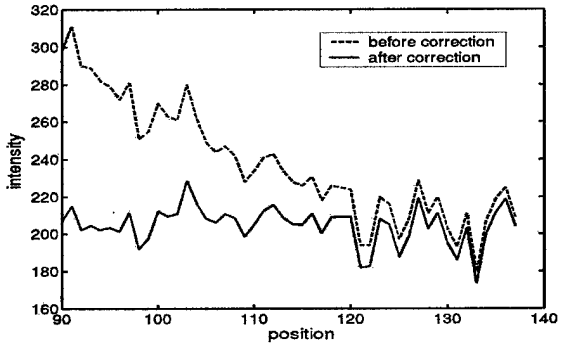

(c)

Fig. 2. Clinical breast MRI example: (a)The orginal image. (b) Corrected image. (c)The intensity profiles of a fat area as marked by a line in (a), for both the original and the bias corrected images.

to original image (a) without considering the bias field effect yielded a membership map shown in Fig.1(e). Apparently, intensity-based segmentation could not correctly segment the image without intensity inhomogeneity correction. By visual evaluation, our algorithm correctly estimated the bias field and dramatically improved the image quality and segmentation accuracy.

Fig.2 presents another breast MRI example. Fig.2(a) and (b) are the original and bias corrected images, respectively. We selected an area mainly consisting of fat tissue and plotted the intensity profiles for both the original and the bias corrected images, as shown in Fig.2(c). From the intensity profile of the original image, we can see that the intensity inhomogeneity in our clinical database can be as large as 40%. From the corrected intensity profile, the algorithm has successfully removed the bias field.

In both examples shown above, the algorithm converged

within 1-2 seconds on a PC AMD Athlon with 1.2 GHz CPU speed.

IV. Discussion

We are developing a computer-aided diagnosis (CAD) system for breast MR imaging. Bias field correction is a necessary preprocessing step for subsequent computerized quantitative analysis. And since the CAD system will ultimately be used in a clinical environment,it must run efficiently. Due to the high spatial resolution and 3-D nature of MR images, we are also using MR images to estimate the percentage of dense tissues in the whole breast, which is an indicator for breast cancer risk. The risk assessment application requires segmentation of the images into different tissue classes in the presence of intensity homogeneity. All these applications motivated us to develop a reliable, fast, and robust algorithm to solve the bias field correction problem.

Our preliminary experiences with the proposed algorithm showed that it is a promising method for intensity inhomogeneity correction and fuzzy segmentation of MR images. Our work in progress includes optimization of the current implementation and evaluation of the method with more data. The noise sensitivity of the algorithm will also be investigated and the neighborhood regularizer as proposed by Ahmed[9] might be incorporated into the current framework to improve the segmentation accuracy on noisy images. Finally, the current version of algorithm works for 2-D images and it is straightforward to generalize to 3-D images.

V. Conclusion

We have presented a fast algorithm based on FCM for intensity inhomogeneity correction and segmentation of MR images. The algorithm was formulated by introducing the bias field model into the FCM objective function which is then minimized iteratively. In each iteration step, the bias field was estimated based on the current tissue class centroids and the membership values of the voxels and then smoothed by an iterative mean filter. The efficacy of the algorithm is demonstrated on clinical breast MR images.

Acknowledgment

The research was supported by DOD Breast Cancer Research Program DAMD17-03-1-0245 and USPHS grant CA89452. M. L. Giger is a shareholder in R2 Technology, Sunnyvale, CA. It is the policy of the University of Chicago that investigators disclose publicly actual or potential significant financial interests that may appear to be affected by the research activities.

References

[1] J. C. Weinreb, G. Newstead,"MR imaging of the breast," *Radiology*,196(3), pp. 593-610, Sept. 1995.

[2] W. M. Kristoffersen, P. Aspelin, M. Sylvan, and B. Bone, "Comparison of lesion size estimated by dynamic MR imaging, mammography and histopathology in breast neoplasms," *Eur Radiol.*,13(6), pp. 1207-12, June 2003.

[3] K. Turetschek, A. Preda, E. Floyd, D. M. Shames, V. Novikov.T. P. Roberts, J. M. Wood, Y. Fu, W. D. Carter. and R. C. Brasch. "MRI monitoring of tumor response following angiogenesis inhibition in an experimental human breast cancer model," *Eur J Nucl Med Mol Imaging*,30(3), pp. 448-55, Mar 2003.

[4] N. A. Lee, H. Rusinek, J. Weinreb, R. Chandra, H. Toth, C. Singer, G. Newstead, "Fatty and fibroglandular tissue volumes in the breasts of women 20-83 years old: comparison of X-ray mammography and computer-assisted MR imaging," *Am J Roentgenol.*, 168(2), pp. 501-6,Feb. 1997.

[5] B. R. Condon, J. Patterson, and D. Wyper, "Image nonuniformity in magnetic resonance imaging: Its magnitude and methods for its correction," *Br. J. Radiol.*, vol. 60, pp. 83-87, 1987.

[6] W. M. Wells, III, W. E. L.Grimson, R.Kikinis, and F. A.Jolesz, "Adaptive segmentation of MRI data," *IEEE Trans. Med. Imag.*, vol. 15, pp. 429-442, Aug. 1996.

[7] R. Guillemaud and M.Brady, "Estimating the bias field of MR images," *IEEE Trans. Med. Imag.*, vol. 16, pp. 238-251, June 1997.

[8] D. L. Pham and J. L. Prince, "Adaptive fuzzy segmentation of magnetic resonance images," *IEEE Trans. Med. Imag.*, vol. 18, pp. 737-752, Sept. 1999.

[9] M. N. Ahmed, S. M. Yamany, N. Mohamed, A. A. Farag, and T. Moriarty,"A modified fuzzy c-means algorithm for bias field estimation and segmentation of MRI data," *IEEE Trans. Med. Imag.*, vol. 21, pp. 193-199, Mar. 2002.

[10] X. Li, L. Li, H. Lu, D. Chen, and Z. Liang, "Inhomogeneity correction for magnetic resonance images with fuzzy c-means algorithm," *Proc. SPIE*,Vol. 5032,Medical Imaging 2003: Image Processing, San Diego, CA, Feb. 2003, pp. 995-1005.

[11] J. Bezdek, L. Hall, and L. Clarke, "Review of MR image segmentation using pattern recognition," *Med. Phys.*, vol. 20, pp. 1033-1948, 1993.

Computerized assessment of tumor extent in contrast-enhanced MR images of the breast

Weijie Chen, Maryellen Giger, Gillian Newstead, Ulrich Bick, Li Lan

Department of Radiology, University of Chicago

1. Introduction

The purpose of this study is to investigate the use of a fuzzy c-means (FCM) algorithm for the assessment of 3-D tumor extent from contrast-enhanced magnetic resonance images (CE-MRI) of the breast. Our database contained 121 cases (77 malignant and 44 benign cases).

2. Methods

For each case, we initially delineated a cubic volume of interest (VOI) that included the consecutive slices about the 3-D mass lesion. For each voxel in the ROI, the signal intensities at six time-points were automatically divided by the precontrast signal intensity, yielding enhancement curves . The standard fuzzy c-mean (FCM) clustering algorithm was then employed to classify each voxel in the ROI into two classes: lesion and non-lesion. FCM outputs two enhancement prototypes associated with the two classes and the fuzzy memberships of each voxel to these two classes. The enhancement prototype that has higher postcontrast enhancement represents the lesion class. The voxels with larger membership values to the lesion class were labeled as 1 and all others were labeled by 0. A 3-D region labeling was then performed on the binary ROI and the largest region was taken as the segmented lesion. Finally, a 3-D hole-filling operation was performed to include necrotic tissue that may have been excluded from the lesion in previous steps due to low enhancement. The results were compared with those of an experienced radiologist using the overlap measure. Overlap is defined as the volume of the intersection of the radiologist-delineated lesion and the computer-segmented lesion divided by the volume of their union.

3. Results

The mean overlap in 3-D between the results of the computerized segmentation and the results of the radiologist outlining was found to be 0.60 with a standard deviation of 0.14. At an overlap threshold of 0.4, 91% of the 121 cases were correctly segmented. The FCM method performed better than our prior volume growing method which yielded 84% correct segmentation at the overlap threshold of 0.4.

4. Conclusion

The proposed method is promising for accurate, consistent, and efficient assessment of breast tumor extent in contrast-enhanced MR images.